Chinese Science Bulletin

The mean residence time of river water in the Canada Basin

CHEN Min[1,2†], XING Na[1], HUANG YiPu[1,2] & QIU YuSheng[1,2]

[1] Department of Oceanography, Xiamen University, Xiamen 361005, China;
[2] State Key Laboratory of Marine Environmental Science, Xiamen University, Xiamen 361005, China

Seawater was collected from the western Arctic Ocean for measurements of ^{18}O, ^{226}Ra and ^{228}Ra. The fractions of river runoff and sea ice melt-water in water samples were estimated by using $\delta^{18}O$-S-PO* tracer system. The mean residence time of river water in the Canada Basin was calculated based on the relationship between $(^{228}Ra/^{226}Ra)_{A.R.}$ and the fractions of river runoff in the shelf and deep ocean. Our results showed that the river runoff fractions in the Canada Basin were significantly higher than those in the shelf regions, suggesting that the Canada Basin is a major storage region for Arctic river water. ^{228}Ra activity concentrations in the Chukchi shelf and the Beaufort shelf ranged from 0.16 to 1.22 Bq/m^3, lower than those reported for shelves in the low and middle latitudes, indicating the effect of sea ice melt-water. A good positive linear relationship was observed between $(^{228}Ra/^{226}Ra)_{A.R.}$ and the fraction of river runoff for shelf waters, while the $(^{228}Ra/^{226}Ra)_{A.R.}$ in the Canada Basin was located below this regressive line. The low $(^{228}Ra/^{226}Ra)_{A.R.}$ in the Canada Basin was ascribed to ^{228}Ra decay during shelf waters transporting to the deep ocean. The residence time of 5.0—11.0 a was estimated for the river water in the Canada Basin, which determined the time response of surface freshening in the North Atlantic to the river runoff into the Arctic Ocean.

Western Arctic Ocean, river runoff, residence time, ^{228}Ra, ^{226}Ra, ^{18}O

It is currently thought that there are two main ways in which the Arctic Ocean might make impacts on global climate. The first is through its effect on the surface heat balance by changing the local radiation and albedo. The second is through its effect on the global thermohaline circulation by regulating deepwater formation rates in the North Atlantic. Both ways are related to the hydrological cycle in the Arctic Ocean. The freshwater components in the Arctic Ocean help to enhance salt stratification and vertical stability in the upper water column, which allows formation of sea ice. Changes in freshwater components in the Arctic Ocean may influence sea-ice extent and thickness, with consequent impacts on surface albedo and turbulent heat fluxes[1]. The variability of the outflow from the Arctic Ocean may lead to basin-scale shifts in the domains of deep convection and the changes of deepwater formation rates in the North Atlantic[2]. Recent evidence suggested that a widespread and rapid freshening of the deep North Atlantic was observed and meridional overturning circulation was slow down[3,4], which was ascribed to the increase of freshwater outflow from the Arctic Ocean[5]. Knowledge of the freshwater cycling in the Arctic Ocean is important for understanding the response and feedback of the Arctic Ocean to the global change.

Three freshwater sources maintain the freshwater budget in the Arctic Ocean: river runoff, net precipitation (precipitation minus evaporation) and the low-salinity Pacific inflow through the Bering Strait. River runoff is clearly one of the key processes contributing to the Arctic Ocean's freshwater budget. The Arctic Ocean

Received October 12, 2007; accepted November 14, 2007
doi: 10.1007/s11434-008-0077-z
†Corresponding author (email: mchen@xmu.edu.cn)
Supported by the Program for New Century Excellent Talents in University of China (Grant No. NCET-04-0593) and the Chinese First Arctic Expedition Foundation

receives 3300 km^3 per year of freshwater by river runoff[6], equivalent to ~10% of runoff from all the world's rivers. The sea ice and the upper waters of the Arctic Ocean serve as major storage reservoirs of fresh water. However, the sea ice melting during summer will increase the freshwater components in local regions. In order to obtain clear understanding of the driving mechanisms determining freshwater distribution in the Arctic Ocean, it is highly desirable to know the distribution of freshwater from each major source and their dynamics. Since only salinity cannot distinguish various freshwater components, researchers used chemical tracers such as ^{18}O[7,8], alkalinity[9], nutrients (SiO_3^{2-}, PO_4^{3-})[10,11], and trace metal (Ba)[12] to reveal the distribution and behavior of various freshwater components in the Arctic Ocean. It is recognized as the important role of the advection of shelf waters in maintaining the upper halocline in the deep ocean[11,13−17].

These tracer studies have provided a good insight into freshwater distribution in the Arctic Ocean. However, little has been known for the time scale of freshwater transport in the Arctic Ocean. There is a range of geochemical tracers to estimate the residence time of freshwater at limited stations in the Arctic Ocean, including $^3H/^3He$, CFCs, bomb ^3H, and $^{228}Ra/^{226}Ra)_{A.R.}$[18 − 23]. However, the residence times obtained by different geochemical tracers have slight difference in physical meaning due to their different input pathways. A residence time derived from $^3H/^3He$ or CFCs is a measure of the time that has elapsed since the last equilibration of the water parcel with the atmosphere. A residence time estimated from a bomb ^3H source function represents the mean time that has passed since the river runoff fraction was discharged onto the shelf. Unfortunately, bomb ^3H can no longer be used as its runoff has stabilized and the vintage age is no longer specific. Unlike above tracers coming from the atmosphere, ^{228}Ra in seawaters comes from the input of river runoff and the release of shelf sediments. With the increasing distance from the shelf region, ^{228}Ra and $^{228}Ra/^{226}Ra)_{A.R.}$ in seawaters decrease due to the radioactive decay. From the distribution of ^{228}Ra or $^{228}Ra/^{226}Ra)_{A.R.}$, one may estimate the transit time of the water masses since they detached from the shelves. Since the river runoff enters the deep basin through the shelf region, the transit time derived from $^{228}Ra/^{226}Ra)_{A.R.}$ also represents the mean residence time of river water in the deep basin[22, 23]. The advantage of $^{228}Ra/^{226}Ra)_{A.R.}$ method over $^3H/^3He$ and CFCs is that the input function of ^{228}Ra from the shelf is irrespective of ice conditions.

In this study, seawater was collected from the western Arctic Ocean during the First Chinese Arctic Expedition for measurements of ^{18}O, ^{226}Ra and ^{228}Ra. The fractions of river runoff and sea ice melt-water in water samples were estimated by using $\delta^{18}O$-S-PO* tracer system. The mean residence time of river water in the Canada Basin was estimated based on the relationship between $^{228}Ra/^{226}Ra)_{A.R.}$ and the fraction of river runoff in the shelf and the deep ocean. The time lag between the maximum river runoff in the Arctic Ocean and the water freshening in the North Atlantic was discussed.

1 Materials and methods

1.1 Sample collection

During July-August, 1999, water samples were collected at 13 stations in the western Arctic Ocean onboard the *R/V* Xuelong. Sampling stations covered the Chukchi shelf (9 stations), the Beaufort shelf (station C30 and C33), and the southern Canada Basin (station C34 and C39) (Figure 1). Water samples were collected from the depth shallow than 500 m at station C34 and C39, and only surface water samples were collected at the other stations.

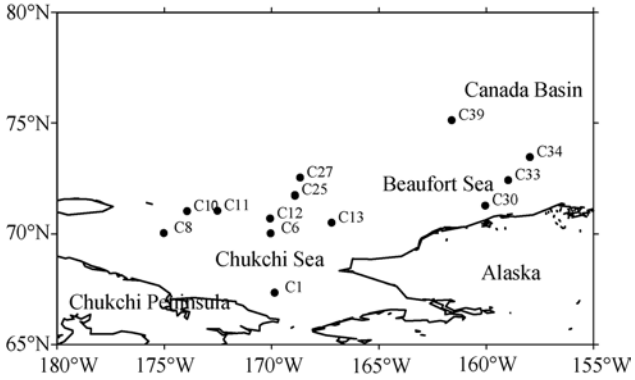

Figure 1 Sampling locations in the western Arctic Ocean.

Seawater for ^{18}O determination was collected using Niskin bottles mounted on a rosette together with a CTD profiler. Surface water samples (120 dm^3) for radium isotopes analysis were collected at ~0.5 m depth with a plastic bucket and passed through a column packed with 12 g MnO_2-fiber. Flow rate of 200−250 cm^3/min was arranged in order to absorb radium isotopes quantitatively. After the enrichment, MnO_2-fiber was taken out

and enveloped in a plastic bag, and taken back to the onshore laboratory for radium analysis. At station C34 and C39 in the Canada Basin, radium samples at different depths were collected by hanging MnO_2-fiber at 25, 50, 100, 150 (or 300), 200 and 500 m for 8—12 h. Since the water volume passing through the MnO_2-fiber was unknown, the activity concentrations of ^{226}Ra and ^{228}Ra can not be obtained, however, the $^{228}Ra/^{226}Ra)_{A.R.}$ in these samples was accurate due to the same water volumn for ^{226}Ra and ^{228}Ra.

1.2 ^{18}O determination

Seawater for ^{18}O determination was filled into a 50 cm^3 plastic bottle and sealed until onboard analysis was conducted. The analytical method for $^{18}O/^{16}O$ ratios was the standard H_2O-CO_2 ^{18}O isotope equilibration technique[15]. Samples were prepared and run in batches, including a national standard and a SLAP standard previously calibrated by direct measurement against Vienna Standard Mean Ocean Water (VSMOW). All analyses were conducted on a VG SIRA-24 isotope ratio mass spectrometer. Analytical uncertainty for oxygen isotope measurements was within ±0.1‰. ^{18}O data reported here were delta values (δ) given in per mil:

$$\delta^{18}\mathrm{O} = \left(\frac{R_{\mathrm{sample}}}{R_{\mathrm{standard}}} - 1 \right) \times 1000 ,$$

where R_{sample} and R_{standard} represent the measured isotope ratios of $^{18}O/^{16}O$ in seawater samples and VSMOW, respectively.

1.3 ^{226}Ra and ^{228}Ra determination

^{226}Ra activity was measured by ^{222}Rn emanation method. In brief, MnO_2-fiber was filled into a diffusion tube, sealed and vacuumized. After 5—7 d, ^{222}Rn produced from ^{226}Ra decay was emanated into a ZnS counting cell, and subsequently measured by a Rn-Th analyzer (FD-125 model, Beijing Nuclear Instrument Factory)[24]. Measurement of ^{228}Ra involved isolation and β counting of the short-lived ^{228}Ac ($T_{1/2}$=6.13 h) following the method described in detail by Xie et al.[24]. As an examination of the radiochemical purity of the isolated ^{228}Ac, radioactive decay curves of ^{228}Ac with the half-lives of 6.11h, 6.14h and 6.45h were derived for samples collected from station C12, C27 and C34-50 m respectively, in good agreement with the accepted value of 6.13h. Therefore, the analytical procedure adopted for ^{228}Ra is reliable. All of the reported ^{226}Ra and ^{228}Ra activity concentrations here were corrected for the equipment background, the blank and the recovery during our procedure, and corrected to the mid-point of the sampling. The reported errors for radium activities were propagated from the one sigma counting uncertainty.

1.4 Measurements of temperature, salinity, phosphate and dissolved oxygen

Temperature and salinity were measured *in situ* by conductivity-temperature-depth instrument (MARK III C/WOCE-CTD), which was calibrated before the cruise[16]. Phosphate and dissolved oxygen concentrations were measurement shortly after the sampling collection. Phosphate concentrations were measured by ammonium molybdate/ascorbic acid method with GBW 08623 as a standard solution[25]. Dissolved oxygen was determined using Winkler technique with GBW 08621 as a standard solution[25]. Analytical uncertainties for phosphate and dissolved oxygen were 0.01 μmol/dm^3 and 0.5 μmol/dm^3, respectively.

2 Results and discussion

2.1 Fractions of river runoff and sea ice melt-water

S-δ^{18}O-PO* tracer system was used to estimate the fractions of the Atlantic water, Pacific water, river runoff and sea ice melt-water in our water samples as described in detail by Chen et al.[15]. The mass balance equations are as follows:

$$f_{\mathrm{a}} + f_{\mathrm{p}} + f_{\mathrm{r}} + f_{\mathrm{i}} = 1, \quad (1)$$

$$f_{\mathrm{a}} \cdot S_{\mathrm{a}} + f_{\mathrm{p}} \cdot S_{\mathrm{p}} + f_{\mathrm{r}} \cdot S_{\mathrm{r}} + f_{\mathrm{i}} \cdot S_{\mathrm{i}} = S_{\mathrm{m}}, \quad (2)$$

$$f_{\mathrm{a}} \cdot \delta^{18}\mathrm{O}_{\mathrm{a}} + f_{\mathrm{p}} \cdot \delta^{18}\mathrm{O}_{\mathrm{p}} + f_{\mathrm{r}} \cdot \delta^{18}\mathrm{O}_{\mathrm{r}} + f_{\mathrm{i}} \cdot \delta^{18}\mathrm{O}_{\mathrm{i}} = \delta^{18}\mathrm{O}_{\mathrm{m}}, \quad (3)$$

$$f_{\mathrm{a}} \cdot \mathrm{PO}^*_{\mathrm{a}} + f_{\mathrm{p}} \cdot \mathrm{PO}^*_{\mathrm{p}} + f_{\mathrm{r}} \cdot \mathrm{PO}^*_{\mathrm{r}} + f_{\mathrm{i}} \cdot \mathrm{PO}^*_{\mathrm{i}} = \mathrm{PO}^*_{\mathrm{m}}, \quad (4)$$

where f_{a}, f_{p}, f_{r}, f_{i} are fractions of the Atlantic water, Pacific water, river runoff and sea ice melt-water contributing to the measured (subscript m) water samples. S_x, $\delta^{18}O_x$ and PO^*_x are the corresponding salinity, δ^{18}O and PO* concentrations ($PO^*=PO_4^{3-}+O_2/175-1.95$ μmol/dm^3 [11]). To conduct the mass balance calculation, a representative concentration for each tracer must be known for each water mass before it enters the Arctic Ocean. The end member characteristics in this study was chosen as the same as previous reported[15]. It should be noted that the calculated fractions of the sea ice melt-water might be positive or negative values. Positive values of the sea ice melt-water fractions meant the net sea ice melting, while negative values represented the portion of freshwater used to form sea ice.

Table 1 shows the calculated fractions of the river

Table 1 ^{228}Ra concentrations, ^{228}Ra/^{226}Ra)$_{A.R.}$ and the fractions of river runoff and sea ice melt-water in the western Arctic Ocean

Region	Station	Longitude (W)	Latitude (N)	Depth (m)	Layer (m)	T (℃)	S	^{228}Ra [a)] (Bq/m^3)	^{228}Ra/^{226}Ra)$_{A.R.}$	f_i (%)	f_r (%)
Chukchi shelf	C1	169°49.5′	67°18.7′	47	0	6.123	31.852	0.61±0.05	0.67±0.06	3.2	6.8
	C6	170°0.6′	69°59.9′	50	0	0.725	25.633	0.35±0.07	1.25±0.27	22.9	5.9
	C8	174°59.5′	70°0.7′	60	0	2.954	31.147	0.25±0.10	0.74±0.29	7.1	5.4
	C10	173°54.3′	71°0.1′	35	0	1.155	26.669	0.54±0.01	1.25±0.09	20.4	5.9
	C11	172°29.6′	71°1.3′	38	0	–1.269	30.500	0.16±0.05	0.56±0.20	7.6	5.3
	C12	170°2.1′	70°40.1′	30	0	–0.876	30.520	0.76±0.06	0.65±0.05	6.7	5.4
	C13	167°10.2′	70°28.8′	50	0	–0.001	31.021	0.41±0.07	0.32±0.05	6.6	2.6
	C25	168°52.6′	71°42.0′	50	0	–0.319	29.099	0.19±0.06	0.68±0.24	12.3	5.7
	C27	168°38.2′	72°29.6′	54	0	–0.974	30.291	1.22±0.09	0.78±0.06	7.2	4.4
Beaufort shelf	C30	160°0.6′	71°15.3′	44	0	1.104	29.850	0.62±0.05	1.19±0.17	6.6	7.0
	C33	158°56.5′	72°22.5′	50	0	0.379	28.395	0.95±0.08	1.09±0.10	9.2	10.0
Canada Basin	C34	157°55.9′	73°25.2′	2700	0	–1.186	26.409	0.55±0.04	0.46±0.04	12.3	12.4
					25	–1.100	29.616	n.d	0.50±0.03	–1.8	14.9
					50	–1.016	31.769	n.d	0.53±0.03	–4.6	10.8
					100	–1.510	32.514	n.d	0.49±0.02	–3.3	7.0
					150	–1.509	33.027	n.d	0.33±0.02	–2.1	4.0
					200	–0.974	33.975	n.d	0.28±0.01	–0.9	2.7
					500	0.470	34.823	n.d	0.08±0.02	1.5	0
	C39	161°55.3′	75°16.1′	2080	0	–1.329	28.295	0.54±0.04	0.58±0.05	3.1	15.7
					25	–0.944	29.382	n.d	0.64±0.06	–0.1	15.7
					50	–0.732	31.642	n.d	0.67±0.07	–6.4	13.9
					100	–1.396	32.590	n.d	0.36±0.04	–3.5	10.9
					200	–1.013	33.990	n.d	0.24±0.01	–1.7	5.3
					300	0.410	34.694	n.d	0.12±0.03	0.8	2.0
					500	0.569	34.823	n.d	0.26±0.02	–0.5	2.7

n.d represents no data.

runoff and sea ice melt-water in studied samples. The fractions of the river runoff in the Canada Basin were significantly higher than those in the Chukchi shelf and the Beaufort shelf, indicating that most of the fresh water transported from rivers was stored in the Canada Basin and the Canada Basin served as a major storage region for river water in the Arctic Ocean[15,26]. The influx of the river water into the Canada Basin was attributed to the large-scale circulation in the Arctic Ocean. The anticyclonic circulation system in the Beaufort Gyre enhanced the gathering of the river runoff to the Canada Basin. The spatial distribution of the sea ice melt-water showed that the surface waters in the Chukchi shelf contained a relatively high fraction of sea ice melt-water, which was ascribed to the geographical south location and the inflowing water from the Pacific. Profiles of the sea ice melt-water fractions at two stations in the Canada Basin showed that positive values were only found in the surface water, indicating a net sea ice melting at the surface and a net sea ice formation below (Table 1).

2.2 ^{228}Ra activity concentrations and ^{228}Ra/^{226}Ra)$_{A.R.}$

Our results showed that surface ^{228}Ra activity concentrations in the western Arctic Ocean ranged from 0.16 to 1.22 Bq/m^3 with an average of 0.55 Bq/m^3 (Table 1). The surface ^{228}Ra concentrations at two stations in the Canada Basin varied a little due to the far distance from the continental. High ^{228}Ra signals were found in the Beaufort shelf resulted from Mackenzie River runoff and the input from the bottom sediments. The surface ^{228}Ra concentrations in the Chukchi shelf varied to a great extent due to the combined impact of the bottom sediments and the sea ice melt-water. On the one hand, ^{228}Ra in the shelf waters will be evaluated by the released from the shelf sediments via pore-water, on the other hand, ^{228}Ra in the shelf waters will be diluted by sea ice melt-water with low ^{228}Ra signals. Our results showed that the fractions of the sea ice melt-water in the Chuckchi shelf varied a great depending on their locations (Table 1). As a result, ^{228}Ra concentrations diluted by sea ice melt-water in the Chukchi shelf varied a great at different locations. In general, ^{228}Ra activity concentrations in the Chukchi shelf and the Beaufort shelf were lower than those reported for shelves in the low and middle latitudes[27], resulting from the effect of the sea ice melt-water. In contrast, ^{228}Ra activity concentrations in the Canada Basin were higher than those in the Pacific Ocean, the Atlantic Ocean and the Indian Ocean[28],

indicating a relatively rapid replenishment of radium from the continental shelves in this high latitude basin.

Surface $^{228}Ra/^{226}Ra)_{A.R.}$ in our study areas ranged from 0.32 to 1.25 with an average of 0.79. The maximal $^{228}Ra/^{226}Ra)_{A.R.}$ was observed at station C6 and station C10 with a low salinity, while the minimal value was at station C13 with a high salinity (Table 1). A negative linear relationship was observed between the surface $^{228}Ra/^{226}Ra)_{A.R.}$ and salinity for shelf waters (Figure 2). However, The surface $^{228}Ra/^{226}Ra)_{A.R.}$ for the Canada Basin stations plotted versus salinity fall below above mixing line for shelf waters due to the decay of ^{228}Ra during the water transport from the shelvies to the deep basin (Figure 2). All of the surface $^{228}Ra/^{226}Ra)_{A.R.}$ in the Chukchi shelf and the Beaufort shelf were lower than 1.25 with an average of 0.84. These results were consistent with previous reported data at two stations in the Chukchi shelf and three stations in the Beaufort shelf ($^{228}Ra/^{226}Ra)_{A.R.}$ = 0.65—1.01) [29], but lower than those observed in the Laptev shelf ($^{228}Ra/^{226}Ra)_{A.R.}$ =3.6) [22]. Profiles of $^{228}Ra/^{226}Ra)_{A.R.}$ at station C34 and C39 in the Canada Basin showed a typical characteristics of $^{228}Ra/^{226}Ra)_{A.R.}$ in the open ocean, with a uniform concentration in the upper mixed layers (0—50 m) and then decreased with the increasing depth (Figure 3).

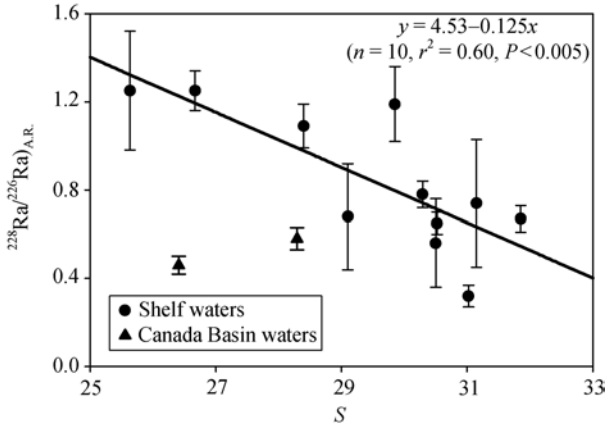

Figure 2 Relationship between surface $^{228}Ra/^{226}Ra)_{A.R.}$ and salinity in the western Arctic Ocean.

2.3 Residence time of the river water in the Canada Basin

^{228}Ra are introduced into the western Arctic Ocean by the inputs of river runoff and the release from the shelf sediments. Since the river water is firstly transported into the coastal regimes, the shelf regions are considered as ^{228}Ra sources for the central Arctic Ocean. In the salinity range investigated, the shelf and river sources cannot be distinguished, and the shelf source of ^{228}Ra can be described by extrapolation as a virtual freshwater source. For the Canada Basin, their ^{228}Ra signals come from the water outflow from the Chukchi shelf and the Beaufort shelf. On the way from the shelf to the Canada Basin, the signal produced in the upper water column by freshwater and shelf inputs is gradually diluted by mixing with underlying water masses, which are depleted in ^{228}Ra. In a plot of $^{228}Ra/^{226}Ra)_{A.R.}$ versus river water fractions in the Chukchi shelf and the Beaufort shelf, a positive linear relationship was observed (Figure 4), indicating the water mass followed the mixing line as long as a constant source concentration and the transport was rapid compared to ^{228}Ra decay. However, $^{228}Ra/^{226}Ra)_{A.R.}$ in the upper 500 m water column in the Canada Basin fall well below this mixing line (Figure 4), reflecting the degree to which ^{228}Ra had decayed during its transport

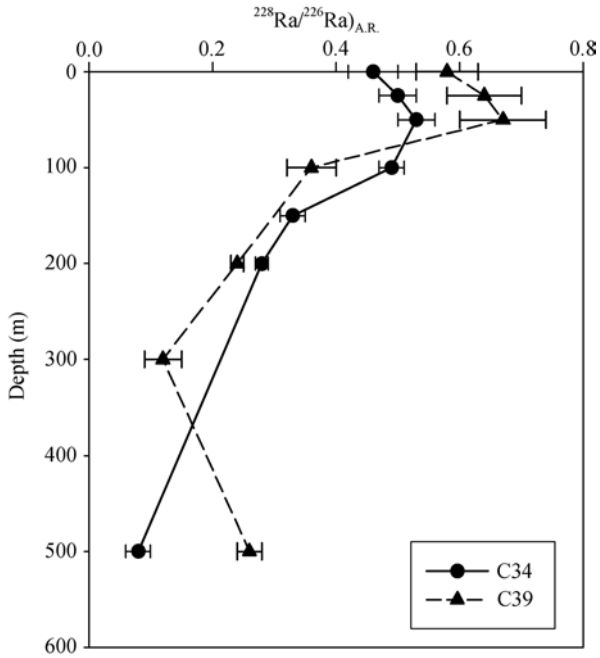

Figure 3 $^{228}Ra/^{226}Ra)_{A.R.}$ profiles in the Canada Basin.

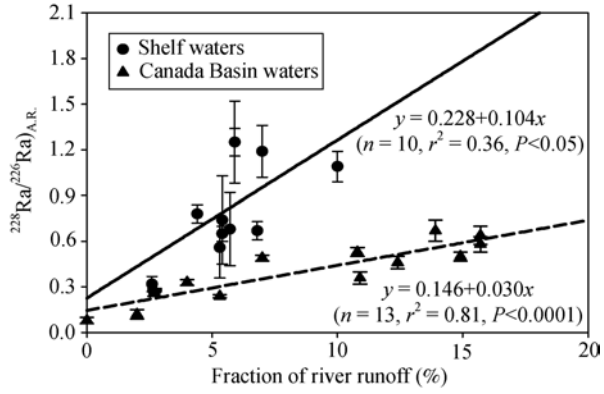

Figure 4 Relationship between $^{228}Ra/^{226}Ra)_{A.R.}$ and the fractions of river runoff in the western Arctic Ocean.

into the interior of the Canada Basin. Based on the angle enveloped by the shelf mixing line and the $^{228}Ra/^{226}Ra)_{A.R.}$ in the Canada Basin, the transit time of the shelf water to the Canada Basin was calculated as

$$\left.\frac{^{228}Ra}{^{226}Ra}\right)^{m}_{A.R.} = \left.\frac{^{228}Ra}{^{226}Ra}\right)^{model}_{A.R.} e^{-(\lambda_{228}-\lambda_{226})t},$$

where $\left.\frac{^{228}Ra}{^{226}Ra}\right)^{m}_{A.R.}$ represents the measured $^{228}Ra/^{226}Ra$ activity ratios in the Canada Basin, $\left.\frac{^{228}Ra}{^{226}Ra}\right)^{model}_{A.R.}$ represents the modeled ratios derived from the shelf mixing line depicted in Figure 4. λ_{228} (0.1205 a^{-1}) and λ_{226} (4.3×10^{-4} a^{-1}) represent the radioactive decay constants for ^{228}Ra and ^{226}Ra respectively, t calculated from above equation is the transit time of water mass from the shelf to the deep basin, which represents the mean residence time of river water in the Canada Basin.

The calculated residence times of the river water were 5.0－10.5 a and 5.6－11.0 a at station C34 and station C39 respectively (Table 2).There was no significant difference of the residence times of river water in the upper mixed layers between both stations, with the average values of 9.4 a (C34) and 8.7 a (C39). However, the residence times of river water in the upper halocline were different at both stations. The mean residence time of river water in the upper halocline at station C34 (5.4 a) was shorter than that at station C39 (10.5), indicating a relatively rapid renewal of river water at station C34.

Table 2 The mean residence time of the river water in the Canada Basin

Station	Depth (m)	$\left.\frac{^{228}Ra}{^{226}Ra}\right)^{model}_{A.R.}$	$\left.\frac{^{228}Ra}{^{226}Ra}\right)^{m}_{A.R.}$	Residence time (a)
C34	0	1.52	0.46±0.04	9.9±0.8
	25	1.78	0.50±0.03	10.5±0.5
	50	1.35	0.53±0.03	7.8±0.4
	100	0.96	0.49±0.02	5.6±0.3
	150	0.64	0.33±0.02	5.5±0.5
	200	0.51	0.28±0.01	5.0±0.3
	500	0.23	0.08±0.02	8.8±2.3
C39	0	1.86	0.58±0.05	9.7±0.7
	25	1.86	0.64±0.06	8.9±0.8
	50	1.67	0.67±0.07	7.6±0.9
	100	1.36	0.36±0.04	11.0±1.0
	200	0.78	0.24±0.01	9.8±0.3
	300	0.44	0.12±0.03	10.8±2.4
	500	0.51	0.26±0.02	5.6±0.7

The mean residence times of river water in the Canada Basin we obtained were consistent with a few previously reported values. Smith et al.[29] estimated a residence time of 10－12 a for the river water in the upper 230 m water column at T3 ice station (84°N, 85°W) in the Canada Basin based upon the relationship between $^{228}Ra/^{226}Ra)_{A.R.}$ and the river water fraction. Hansell et al.[23] reported a residence time of 7－13 a for the surface water in the Beaufort slope according to their measured $^{228}Ra/^{226}Ra)_{A.R.}$ in the Beaufort Sea and the relationship between $^{228}Ra/^{226}Ra)_{A.R.}$ and salinity in the Transport Drift. Östlund[21] compared the time functions of bomb ^{3}H concentrations in the river runoff to the Arctic Ocean and the time series data of ^{3}H concentrations in the Arctic Ocean, and a residence time of 9－17 a was estimated for the river water in the upper 100－400 m water column. Besides, the mean residence time of river water in the Arctic Ocean has been estimated by Bauch et al.[30] from $\delta^{18}O$ mass balance calculations to be 11－15 a.

A mean residence time of ~10 a for the river water in the Arctic Ocean was assessed according to our results and previous reported data, indicating that river water added to the Arctic Ocean will be flushed out of the system on time scales of about 10 a. This value was useful for understanding the time-series variability of salinity in the deep water formation regions in the North Atlantic. Dickson et al.[31] depicted the time-series change of salinity from 1950 to 1999 in the upper 2000 m water column in the Norweigian Sea. From which one may find that salinity was decreased in 1958－1959, 1967, 1977－1981, 1984－1985 and 1994－1999. It is interesting to note that the river runoff into the Arctic Ocean was at maximum in 1947－1949, 1958, 1966－1968, 1974－1978 and 1986－1988[32]. The time intervals between the freshening of the North Atlantic and the maximum river runoff to the Arctic Ocean were 10a, 9a, 12a, 9a and 9a respectively, which were well consistent with the mean residence time of river water in the Arctic Ocean. Obviously, the water freshening in the upper layer of the North Atlantic was related to the increased river runoff to the Arctic Ocean, and the response time in the North Atlantic was about 10a later after the increased river runoff in the Arctic Ocean.

3 Conclusion

Based on the δ^{18}O-S-PO* tracer system, the fractions of river runoff in the Canada Basin were significantly higher than those in the Chukchi shelf and the Beaufort shelf, testifying that the Canada Basin is a major storage for river waters in the Arctic Ocean. ^{228}Ra activity concentrations in the Chukchi shelf and the Beaufort shelf were lower than those reported for shelves in the low and middle latitudes, attributing to the effect of sea ice melt-water. According to the relationship between ^{228}Ra/^{226}Ra)$_{A.R.}$ and the fractions of river runoff in the shelf and the deep basin, a mean residence time of 5.0－11.0 a of river water in the Canada Basin was estimated. The estimated residence time of river water was consistent with the time lag between the increase of the Arctic river runoff and the water freshening in the North Atlantic.

This work could not be possible without the assistance of the officers and crew of the R/V XUELONG. The authors wish to thank Zhao Jinping, Gao Guoping and Jiao Yutian for providing the CTD data, Jin Mingming and Lu Yong for providing nutrients data, and two anonymous reviewers for constructive comments.

1 Carmack E C. The Arctic Ocean's freshwater budget: sources, storage and export. In: Lewis E L, Jones E P, Lemke P, et al. eds. The freshwater budget of the Arctic Ocean. Dordrecht: Kluwer Academic Publishers, 2000. 90－126
2 Aagaard K, Carmack E C. The Arctic and climate: a perspective. Geophys Monogr Ser, 1994, 85: 4－20
3 Dickson B, Yashayaev I, Meincke J, et al. Rapid freshing of the deep North Atlantic Ocean over the past four decades. Nature, 2002, 415: 832－837
4 Bryden H L, Longworth H R, Cunningham S A. Slowing of the Atlantic meridional overturning circulation at 25°N. Nature, 2005, 438: 655－657
5 Clark P U, Marshall S J, Clarke G K C, et al. Freshwater forcing of abrupt climate change during the last glaciation. Science, 2001, 293: 283－287
6 Aagaard K, Carmack E C. The role of sea ice and other fresh water in the Arctic circulation. J Geophys Res, 1989, 94: 14485－14498
7 Östlund G, Hut G. Arctic Ocean water mass balance from isotope data. J Geophys Res, 1984, 89: 6373－6381
8 Schlosser P, Newton R, Ekwurzel B, et al. Decrease of river runoff in the upper waters of the Eurasian Basin, Arctic Ocean, between 1991 and 1996: evidence from δ^{18}O data. Geophys Res Lett, 2002, 29(9), 1289, doi: 10.1029/2001GL013135
9 Anderson L G, Jutterstrom S, Kaltin S, et al. Variability in river runoff distribution in the Eurasian Basin of the Arctic Ocean. J Geophys Res, 2004, 109, C01016, doi: 10.1029/2003JC001773
10 Jones E P, Anderson L G, Swift J H. Distribution of Atlantic and Pacific waters in the upper Arctic Ocean: implications for circulation. Geophys Res Lett, 1998, 25: 765－768
11 Ekwurzel B, Schlosser P, Mortlock R, et al. River runoff, sea ice meltwater, and Pacific water distribution and mean residence times in the Arctic Ocean. J Geophys Res, 2001, 106: 9075－9092
12 Guay C K, Falkner K K. Barium as tracer of Arctic halocline and river water. Deep-Sea Res II, 1997, 44: 1543－1569
13 Aagaard K, Coachman L K, Carmack E C. On the halocline of the Arctic Ocean. Deep-Sea Res, 1981, 28: 529－545
14 Jones E P, Anderson L G. On the origin of the chemical properties of the Arctic Ocean halocline. J Geophys Res, 1986, 91: 10759－10767
15 Chen M, Huang Y P, Jin M M, et al. The sources of the upper and lower halocline water in the Canada Basin derived from isotopic tracers. Sci China Ser D - Earth Sci, 2003, 46(6): 625－639
16 Shi J X, Zhao J P, Li S J, et al. A double-halocline structure in the Canada Basin of the Arctic Ocean. Acta Oceanol Sin, 2005, 24(6): 25－35
17 Yamamoto-Kawai M, Tanaka N. Freshwater and brine behaviors in the Arctic Ocean deduced from historical data of δ^{18}O and alkalinity (1929－2002 A.D.). J Geophys Res, 2005, 110, C10003, doi: 10.1029/2004JC002793
18 Schlosser P, Bonisch G, Kromer B, et al. Ventilation rates of the waters in the Nansen Basin of the Arctic Ocean derived from a multitracer approach. J Geophys Res, 1990, 95: 3265－3272
19 Wallace D W R, Schlosser P, Krysell M, et al. Halocarbon ratio and tritium/^{3}He dating of water masses in the Nansen Basin, Arctic Ocean. Deep-Sea Res, 1992, 39: S435－S458
20 Krysell M, Wallace D W R. Arctic Ocean ventilation studied with a suite of anthropogenic halocarbon tracers. Science, 1988, 242: 746－749
21 Östlund H G. The residence time of the freshwater component in the Arctic Ocean. J Geophys Res, 1982, 87(C3): 2035－2043
22 Rutgers van der Loeff M M, Key R M, Scholten J, et al. ^{228}Ra as a tracer for shelf water in Arctic Ocean. Deep-Sea Res II, 1995, 42(6): 1533－1553
23 Hansell D A, Kadko D, Bates N R. Degradation of terrigenous dissolved organic carbon in the western Arctic Ocean. Science, 2004, 304: 858－861
24 Xie Y Z, Huang Y P, Shi W Y, et al. Simultaneous concentration and determination of ^{226}Ra, ^{228}Ra in natural waters. J Xiamen University (Natural Sci) (in Chinese), 1994, 33(Suppl): 86－90
25 Jin M M, Shi J X, Lu Yong, et al. Nutrient maximums related to low oxygen concentrations in the southern Canada Basin. Acta Oceanol Sin, 2005, 24(6): 88－96
26 Serreze M C, Barrett A P, Slater A G, et al. The large-scale freshwater cycle of the Arctic. J Geophys Res, 2006, 111, C11010, doi: 10.1029/2005JC003424
27 Xie Y Z, Huang Y P, Shi W Y, et al. ^{226}Ra and ^{228}Ra in Jiulongjiang estuary area. J Oceanogr in Taiwan Strait (in Chinese), 1994, 13(4): 394－399
28 Kaufman A, Trier R, Broecker W S. Distribution of ^{228}Ra in the world ocean. J Geophys Res, 1973, 78: 8827－8848
29 Smith J N, Moran S B, Macdonald R W. Shelf-basin interactions in the Arctic Ocean based on ^{210}Pb and Ra isotope tracer distributions. Deep-Sea Res I, 2003, 50: 397－416
30 Bauch D, Schlosser P, Fairbanks R. Freshwater balance and the sources of deep and bottom waters in the Arctic Ocean inferred from the distribution of $H_2{}^{18}O$. Prog Oceanogr, 1995, 35: 53－80
31 Dickson R D, Curry R, Yashayaev I. Recent changes in the North Atlantic. Phil Trans R Soc Lond A, 2003, 361: 1917－1934
32 Shiklomanov I A, Shiklomanov A I, Lammers R B, et al. The dynamics of river water inflow to the Arctic Ocean. In: Lewis E L, Jones E P, Lemke P, et al. eds. The Freshwater Budget of the Arctic Ocean. Dordrecht: Kluwer Academic Publishers, 2000. 281－296